

## Different Materials Consisting the Interference Shrink-Fitted Joints

" مواد مختلفة تكون الجلب المتداخلة بالانكماش "  
By

Dr. I. Elewa and Dr. A. Abdel Shafi  
Faculty of Engineering-Mansoura University

خلاصة - كانت المواد المستخدمة في غالبية الأبحاث السابقة والمتعلقة بدراسة خصائص جلب التداخل بالانكماش مواداً من الصلب الطري ( المرن ) المتداول تجارياً . إلا أن وصلات التداخل بالانكماش صنع من مواد مختلفة بما في ذلك المواد الحديدية والغير حديدية منها . وينصب اهتمام البحث الحالي على التأثير الناتج من تغيير نوعية المواد المستخدمة ناهيك عن تأثير استخدام تركيبات مختلفة من المواد على قوة تحمل الجلبة . وقد نحتونا أسلوباً نظرياً بغية حساب قوة تحمل الجلبة وكذا الاجهادات المتولدة بين سطحي التلامس بتلك الجلبة . كما تم وضع خطة عملية لدراسة تأثير بعض العوامل على قوة تحمل الجلبة . كخشونة السطح وقيمة التداخل . أما عن المواد التي استخدمت لانتاج تلك الجلب فهي الصلب الطري والنيحاس الأصفر والالمنيوم والنيحاس الأحمر .

1- Summary: The materials used for the most previous work to investigate the characteristic of shrink-fitted joints are a commercially available mild steel. Shrink-fitted joints are produced using a much wider material range which can include nonferrous materials. The paper at hand is concerned with the effect of changing material type and the use of differing material combinations on the joint holding load.

A theoretical approach is adopted to evaluate the holding load and stress induced between the two mating surfaces of the joint. Also, an experimental work is designed to investigate the effects of some parameters on the joint holding load i.e. the surface roughness and the interference value. The different materials used to produce the two members of the joints are, Mild Steel, Brass, Aluminium, and Bronze Phosphoric Copper.

### 2- Introduction

The fundamental basis of shrink-fit construction as in all types of applications, where residual or initial stresses are purposely induced in the material, is to utilize favorably distributed internal stresses rather than increased weight of material to resist service load. In shrink-fit construction the intent may be to increase the elastic range of material used to increase the fatigue life of the joint. In many instances a low-cost material, weak from the stand-point of inherent strength, can be used in a prestressed condition to accomplish the same results as a more expensive higher-strength material (1,2,3).

Shrink-fit constructions are well suited to many different design situations, such as replaceable liners in pressure vessels or strengthening of a liner by a shrunk-on shell that helps retard crack propagation. Its versatility is also demonstrated in assemblies composed of materials having different properties or degrees of corrosion resistance, such as a shrunk-on steel shaft over a copper or aluminium ring, where maximum utilization is made of the properties of both materials.

It is usual, in the case of an assembly, having shaft and ring, the mating surfaces dependent upon the elastic properties of the materials for its grip, to employ Lame's thick cylinder theory to determine the magnitude of stresses induced in the hollow and solid elements. The theory is so well known in connexion with force and shrink-fits that it needs

only be briefly referred to. It is therefore good practice to make the fit as tight as the properties of the male and female material will permit, i.e. fit which does not allow the circumferential stress in the female bore to exceed the yield strength of the material (4).

The traditional recommendation is to produce a joint with surface as smooth as possible, but this method is limited by the economy of the manufacture of such parts. The sacrifice in economy for uncalculated and indefinite gain in the joint holding load is not an acceptable engineering practice. Consequently, it has been substituted by increasing the joint interference value, which has resulted in the limited use of such fits due to the large stresses induced in the mating parts. Moreover, a large value of interference can have an adverse effect on the holding load if the stresses exceed the material yield stress.

### 3- Theoretical analysis:-

#### 3.1 Effect of material and Heat treatment:-

The experimental results showed that the holding load of a force-fitted joint can be increased by increasing the elastic limit of the material through cold working (4). Conway's (5) attempt to verify Lamé's equation has shown that the two fundamental factors affecting the grip between the two shrink-fitted components are the elastic limit and the magnitude of the modulus of elasticity. It has also been shown that the interference required to give a specific radial pressure is inversely proportional to the Young's modulus. From a comparison between several different materials it becomes obvious, when using Lamé's formula that an increase in the modulus of elasticity is followed by a proportional increase in the holding load. For example, the holding load of a joint made of steel is three times greater than the same joint manufactured from duralumin.

The experimental results have shown that, when materials with comparable tensile strengths need to be selected, it is preferable to choose a material with high toughness and high yield points, because it is on these features that the fatigue strength mainly depends (6). Kestelman (2) has carried out an experimental investigation in which carbon bushings were press-fitted to metal parts. The results have shown that the load which must be supplied to form the joint is dependent on the surface roughness and the heat treatment method. The bushings that are heat treated using oil, require 50% higher force than those treated using water. Oil is a more preferable heat treatment medium due to the improvement in reliability and strength that accompany its use. The strength of the permanent joints increases with increasing the value of interference, of joint length and of bushing wall thickness, as well as of the metal part surface roughness and heat treatment. The tests have also shown that heat treatment of carbon bushings in oil can be used to improve the reliability and strength of the permanent joints.

#### 3.2 Stresses induced in the shrink-fitted joints:-

Fundamentals of shrink-fit theory are covered by analyses of heavy-walled cylinders subjected to internal and external pressure. Fabrication procedures involved, lubrication of shrink-fit assemblies, preparation of contact surfaces and similar manufacturing problems will not be considered here (7)

Cross sections of various types of shrink-fit constructions are; ring and solid shaft under shrink-fit pressure only, ring and hollow shaft under shrink-fit pressure only, two-shell vessel with internal pressure and shrink-fit pressure, and, ring and shaft subjected to shrink-fit pressure and centrifugal forces. In all cases the component parts are not necessarily of the same material.

The simplest case to be considered is when only shrink-fit pressure is taken into account. Two situations will be discussed.

### 3.2.1 Different Materials-Hollow shaft

In the general case, the assembly is a two-part system, each part having different properties. The assembly is held together by a shrink-fit pressure,  $P$ . The outer component has a poisson's ratio of  $\nu_o$  and an elastic modulus of  $E_o$ , and the inner component has a poisson's ratio  $\nu_i$  and an elastic modulus of  $E_i$ .

The radial deformation for the inner cylinder is:

$$\Delta_i = \frac{-P}{E_i} \left( \frac{a^2 + d^2}{d^2 + a^2} - \nu_i \right) d \quad \dots (1)$$

Deformation for the outer component is:

$$\Delta_o = \frac{P}{E_o} \left( \frac{d^2 + D^2}{D^2 - d^2} + \nu_o \right) d \quad \dots (2)$$

The total shrinkage allowance is the absolute sum of the individual deformations;

$$\Delta = Pd \left[ \frac{1}{E_o} \left( \frac{d^2 + D^2}{D^2 - d^2} + \nu_o \right) + \frac{1}{E_i} \left( \frac{a^2 + d^2}{d^2 + a^2} - \nu_i \right) \right] \quad \dots (3)$$

From equation the shrink-fit pressure is:

$$P = \frac{\Delta}{d} \left[ \frac{1}{E_o} \left( \frac{d^2 + D^2}{D^2 - d^2} + \nu_o \right) + \frac{1}{E_i} \left( \frac{a^2 + d^2}{d^2 + a^2} - \nu_i \right) \right] \quad \dots (4)$$

### 3.2.2 Different Materials-Solid Shaft

If the inner component is a solid shaft,  $a=0$  and equations 3 and 4 become:-

$$\Delta = Pd \left[ \frac{1}{E_o} \left( \frac{D^2 + d^2}{D^2 - d^2} \right) + \nu_o + \frac{1 - \nu_i}{E_i} \right] \quad \dots (5)$$

and

$$P = \frac{\Delta}{d \left[ \frac{1}{E_o} \left( \frac{D^2 + d^2}{D^2 - d^2} + \nu_o \right) + \frac{1 - \nu_i}{E_i} \right]} \quad \dots (6)$$

The axial force that a shrink-fit assembly can withstand without separation of the parts is:

$$H.L.F = \pi L d P \dots (7)$$

The paper at hand is concerned with the previous case in which the shaft will be solid and the joint will consist of different materials combination.

### 3.3 Estimation of the joint Holding load using a Theoretical approach

The pressure induced between the two mating surfaces representing every joint is estimated using equation (6). The pressure of every joint is calculated at a different level



of interference value using the mechanical properties (i.e. E &  $\nu$ ) of the materials forming the joint male and female as given in table (1).

Table (1) Mechanical Properties of The Materials used

Mech. prop. Mat. type	E Modulus of Elast. kg / mm <sup>2</sup>	Poisson $\nu$ ratio	Elongation %	BHN	kg/mm <sup>2</sup> ultimate tensile strength
Mild Steel	$2.1 \times 10^4$	0.29	24	120	37
Aluminium Alloy	$0.675 \times 10^4$	0.34	5	95	12
Copper	$1 \times 10^4$	0.32	45	35	18
Brass	$1.25 \times 10^4$	0.37	40	60	22

To evaluate the joint holding load using equation (7), the static coefficient of friction ( $\mu_s$ ) between the two mating surfaces of the joint should be estimated.

The method adopted in the present research is based on estimating the mean slope of the surface profile and by substituting in equation (8), which has been predicted by the theory of dry friction between rough surfaces (8) the value of  $\mu_s$  can be evaluated.

### 3.3.1 The static coefficient of friction $\mu_s$

Hisakada (8-9) has investigated the effect of surface roughness on dry friction between two metals, assuming that the asperities are cones of slopes which depended on the surface roughness. A theoretical expression is derived which includes ploughing and adhesion in determining the friction coefficient for cones, spheres and square pyramids ploughing along a soft metal surface.

Hisakado suggests that the theoretical estimation of the coefficient of friction between two metal surfaces can be determined using the relations between the surface roughness, the slope of the asperities and the coefficient of friction due to the adhesion at the interface.

Tsukizone et al (10) has investigated the effects of surface roughness on the joint holding load of shrink-fitted joints. For the purpose of computing the theoretical and experimental values of the holding load, the static coefficient of friction  $\mu_s$  is estimated by substituting a value of  $\xi_s = 0.7$ ,  $\mu = 0.4$  for rough surfaces and  $\xi_s = 0$ ,  $\mu = 0.193$  for smooth surfaces in the following equation:-

$$\mu_s = \xi_s \mu + (1 - \xi_s) \frac{\frac{2}{\pi} \tan \theta + 0.5 \mu (\frac{1}{\cos \theta} + 1)}{1 - \frac{2}{\pi} \mu \tan \theta} \quad \dots (8)$$

This technique has proved very successful in representing the experimental data.

The paper at hand adopted a similar approach to evaluate the static coefficient of friction  $\mu_s$ . It is considered that an average value of the mean slope depending on the different parameters that characterise the surface, namely,  $R_a$  and the average wave length represent a better estimation of the mean slope. The following equation is used to evaluate the mean slope of every surface forming the joint and these values are shown in tables (2,3,4,5)

$$\tan(\theta) = \frac{2 \pi R_a}{\lambda_a} \quad \dots (9)$$

The average wave length  $\lambda_a$  is calculated using a Talysurf (4) and taken as the average of ten traces obtained at the mean line of profile. By substituting in equation (8) the static coefficient of friction of every surface can be obtained.

The average static coefficient of friction  $\mu_s$  of every joint is calculated and by substituting in equation (7) the holding load of every joint is obtained as shown in tables (2,3,4,5)

#### 4. Experimental Work

##### 4.1 Specimen preparation

The two members of the different joints are manufactured using a mild steel, Brass, Copper, and Aluminium alloy. The joints are divided into four equal groups, according to the material type used, to produce the rings. A large number of rings is manufactured to provide enough specimens for the matching process. The shafts for all groups are manufactured using a mild steel while the rings of the four groups are manufactured using a mild steel, Brass, copper and Aluminium alloy respectively. The mechanical properties of each material used are shown in table (1).

The process used to manufacture all the joints members is a turning process. The process parameters have a significant influence on the surface roughness degree, hence, it is necessary to change the process parameters to produced three different degrees of surface finish.

The nominal size of all joints is 20 mm. (inner diam.) the outer diameter is 50 mm and the height is 20 mm.

##### 4.2. Surface Roughness Measurements:-

Talysurf (4) is used to determine the  $R_a$  value of every shaft and ring as shown in Fig (1). The stylus of the Talysurf is positioned to move along the specimens which are held in a vee-block to obtain the  $R_a$  value across the lay. The mean value of  $R_a$  is taken as the average of ten readings. Also, for each specimen ten readings are taken at the mean line, i.e. the HSC, from which the average wave length is obtained as the quotient of dividing the stroke length by the number of spots.

##### 4.3. Dimensional Measurements:-

The outer diameter of the shaft and the inner diameter of the ring are measured using a Universal Measurescope model (10) which has a scale value of 1  $\mu\text{m}$ , as shown in Fig. (2). Ten readings are obtained for both shaft and ring with the average value taken as the effective diameter.

##### 4.4 Joint Assembly:-

Pair consists of a shaft and a ring of practically the same surface roughness ( $R_a$ ) are chosen to form joints of different interference value and different material type for each group.

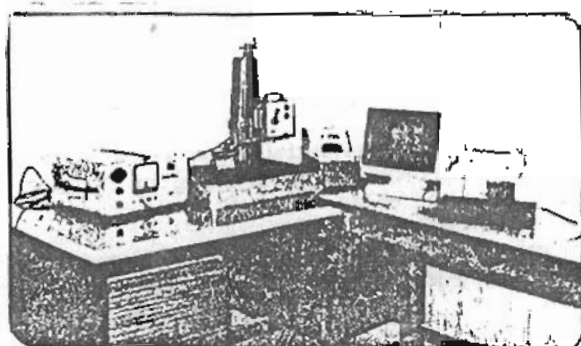


Fig. (1) Surface Roughness Measurements  
(Taly Surf 4)

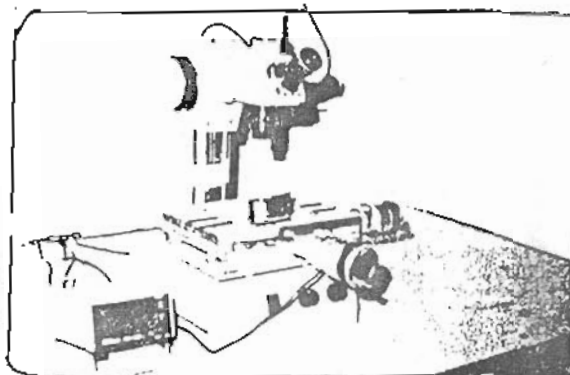


Fig. (2) Dimensional Measurements  
(Measuring Scope 10)

The interference value of each joint is chosen to fulfill the following conditions:-

- i - To provide adequate interference to ensure satisfactory strength for the finish assembly.
- ii - To keep the stresses resulting from the fit below the level of the material allowable stress.
- iii - To ensure that the amount of heating the rings would provide an adequate clearance for fitting.

#### 5. Experimental Investigation:-

The tension tests are carried out using a 30 tons Universal testing Machine, hydraulically operated, the holding load of the joint is obtained directly from the machine dial which has a scale value of 0.01 ton.

The dial calibration is carried out using a proof ring and it was found satisfactory within + 1%.

The load is applied steadily, and as soon as the pointer of dial oscillates, the load is read on the dial and this value is considered as the holding load of the joint under test.

#### 6. Results And Discussion:-

##### 6.1 The effect of surface roughness.

The effects of varying surface roughness  $R_a$  on the joint holding load for all joints types investigated are shown in Fig. (3-6). For all joints types the holding load decreases with increasing the surface roughness  $R_a$ . The rate of increase in the holding load with decreasing the surface roughness  $R_a$  is much greater for the joints made of copper, Brass, Aluminium and Mild steel respectively.

##### 6.2 The effect of interference value:-

Fig. (3-6) show the relationships between the holding load and the interference value for all joints types tested (steel, brass, copper and Aluminium). As can be seen from figures, the general trend can be represented by a linear relationship for the small value of interference. After a certain interference value the relationship starts to show



a non-linear trend. This non-linearity can be directly related to the material elastic behaviour. The low levels of interference are not enough to induce stresses beyond the material-elastic limit, whilst at a high interference levels the stresses may reach the material plastic range. The deviation from linearity for each curve has proved to be material type-dependent. The increases in the joint holding load with the increasing in the interference value is due to the pressure increase induced between the two mating surfaces of the joint. Also, it is clear from figures that the rate of increases in the joints holding load manufactured of mild steel has a largest rate whilst the copper joints has a lowest rate at  $R_a = 1.1 \mu\text{m}$  for an increase of  $40 \mu\text{m}$  in the value of interference.

### 6.3 The effect of material type on the H.L.

The type of material has a significant influence on the holding load value as shown in Fig. ( 3 - 6 ). For the same value on interference and surface roughness the holding load of the joints manufactured of mild steel has the highest value, whilst the Aluminium joints have the lowest value. It is clear from the experimental data that the joint manufactured of material with a largest value of modulus of elasticity has also the largest value of holding load at the same interference and surface roughness value.

It can be seen from the tables, that the percentage deviations of Brass, copper and Aluminium joints holding load from steel joints holding load are, 48%, 52% and 65% respectively at interference value of  $19 \mu\text{m}$ . By increasing the interference value to  $54 \mu\text{m}$ , the percentage deviations become, 72%, 75% and 77% at the same value of surface roughness. This means that the joint holding load is dependent on the material type of produced the joint i.e. the material with a higher value of modulus of elasticity has a largest value of holding load.

### 6.4 Holding load determination (theoretical method).

The details of the method used to include  $\mu_j$  in calculating the theoretical joint holding load are outlined in 3.3. Tables 2 to 5 showed the predicted value of holding load for the experimental range investigated. The main joint parameters, viz, surface roughness and value of interference, all play an important role in determining the degree of correlation between the theoretical and experimental data values.

For mild steel joints the percentage deviation between the theoretical and experimental values has proved to be more closed than in the case of the other types of joints. For small value of joint interference, a small percentage deviation have not increased to more than 35% at  $54 \mu\text{m}$  interference level and  $1.07 \mu\text{m} R_a$  and this deviation increased to 50% at  $R_a = 2.46 \mu\text{m}$  to reach about 100% for  $R_a = 5.56 \mu\text{m}$ .

The percentage deviation for the Brass, copper and Aluminium joints is about 50% for a small value of  $R_a$  and interference level did not increase to more than  $20 \mu\text{m}$ , while this deviation increased rapidly by increasing the value of interference and surface roughness  $R_a$  as shown in tables 2-5.

This method of determining the joint holding load using the coefficient of friction relied on using empirical equation which are based on measuring the physical parameters characterising the surfaces, such as the profile mean slope  $\tan \phi$ . The average mean slope is also dependent on the average wave length and centre line average  $R_a$  and neglects the effect of the geometrical errors i.e. out of straightness and out of roundness in the analysis. The analysis of the experimental results indicates that the results obtained using

this method give a better overall assessment of the experimetal data of the mild steel joints ,whilst they give a good correlation for the other type of joint at small levels of interference and smooth surfaces only. see Fig. (7).

#### Conclusions:-

At higher levels of interference and for rough surfaces factual evidence suggest that the situations may have some resemblance between them and sticking condition at the very edge of the cutting tool tip. An investigation in that direction might miret some considerations is beyond the scope of the present work.

The main results and conclusions can be stated as follows:-

- 1- The joint holding load of shrink-fitted joints which consists of combination materials increases proportionally with the increase in the interference value for the same value of surface roughness  $R_a$ .
- 2- For the same joint surface roughness  $R_a$  the percentage deviations of Brass, copper and Aluminium joint holding load from steel joint H.L. are, 48%, 52% and 65% respectively at interference value of 19  $\mu\text{m}$ . and this % deviation increases by increasing the interference value.
- 3- For a given value of interference, the joint holding load increases with decreasing the joint surface roughness  $R_a$  for all types of joints.
- 4- For the same value of interference and surface roughness  $R_a$ , the joint holding load increases with increasing the modulus of elasticity of the material consisting the joint.
- 5- The theoretical method of estimating the joint holding load using the coefficient of friction us gives a better overall assessment of the experimental data obtained for the mild steel joints, while the data obtained for Brass, copper and Aluminium are reasonable only for smooth surfaces ( $R_a = 1 \mu\text{m}$ ) and small value of interference (20  $\mu\text{m}$ )

#### Appendix A

##### Nomenclature:-

$P_m$	Mean interface pressure
$d$	Joint nominal size
$D$	Outside diameter of the ring
$L$	Length of fit
$\mu_s$	Static coefficient of friction
$E_s$	Youg's Modulus of Elasticity for the ring
$E_i$	Yough's Modulus of Elasticity for the shaft
$\Delta$	Interference on the diameter
$\nu_o$	Poisson's ratio of the ring.
$\nu_i$	Poisson's ratio of the shaft.
$\mu$	Coefficient of friction due to adhesion at the interface
$\epsilon$	The ratio of the normal load supported by the junctions at which adhesion only takes place to the total normal loads
H.L.	Joint Holding load.
$a$	Inner dia. of female component



References :

- 1- BAUGHER J.W. Transmission of torque by means of press and shrink-fit. Trans. ASME, Vol. 53, 1931.
- 2- KESTEL'MAN N.Y, KESTEL'MAN N.V. and MUKHA M.S, Strength of nomoving joints formed beteen carbon bushings and parts. Chem. and petrolum, No. 3-4, 1969, pp 185-187.
- 3- HISAKADO T. and MIYOSHI K, Effect of roundness on shrink-fits. Bull. JSME, Vol. 16, No. 102, 1973, pp. 1977.
- 4- WILSON W.K., The Strength of large crank-shafts. Gas and oil power, Vol. 46, No. 554, 1951.
- 5- CONWAY H.G. Engineering Tolerances. Pitman, London, 1966.
- 6- EUBANKS R.A., Shrink-fit of aritrary length sleeves on thin cylindrical shells. Proc. 8 th Midwestern Mechs. Conf. 2, Part 2, 1963, pp. 84-101.
- 7- I. M. Elewa, "A study of some parameters which influence the static and dynamic characteristics of interference shrink-fitted Joints" Ph. D., Aston Univ., Birmingham, UK., 1982.
- 8- HISAKADO T, On the mechanism of contact solid surfaces, JSME, Vol. 13, No. 55, 1970, pp 129-139.
- 9- TSUKIZOE T. and HISAKADO T. The influence of surface roughness on the mechanism of frication. Trans. Am. Soc. Mech. Engrs., Vol. 92, Ser. F, 1970.
- 10- TSUKIZOE T., HISAKADO T. and MIYOSHI K, Effects of surface roughness on shrink-fits. Bull. of the JSME, Vol. 17, No. 105, 1974.

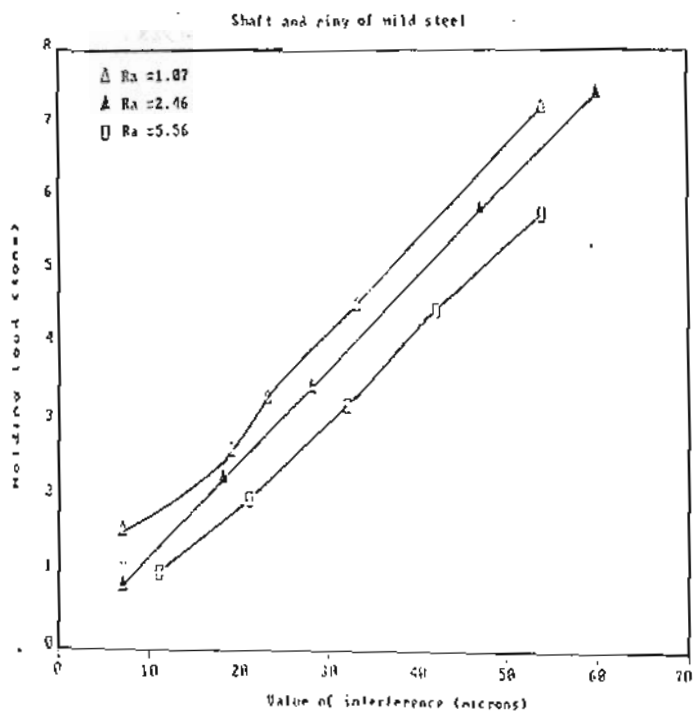


Fig. 3: Effect of the interference value on the H.L. of Mild steel joints.

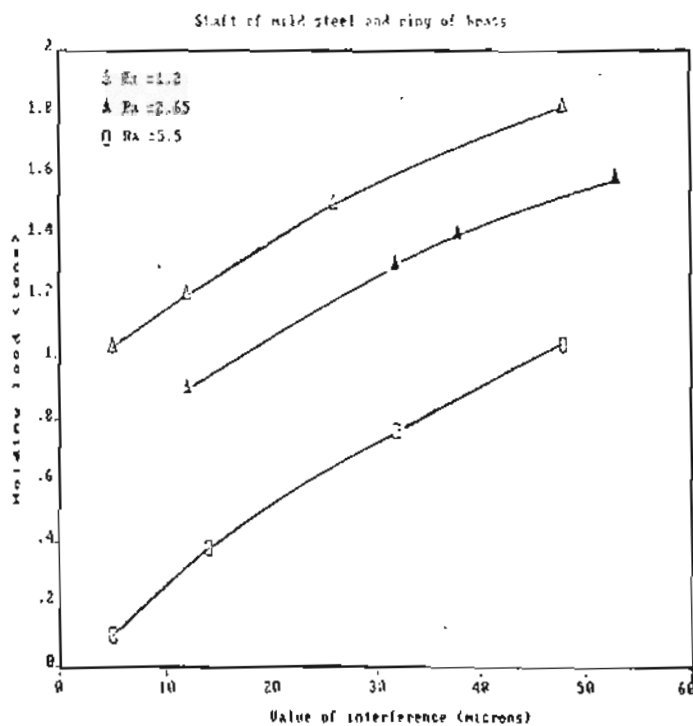


Fig. 4: Effect of the interference value on the H.L. of Brass joints .

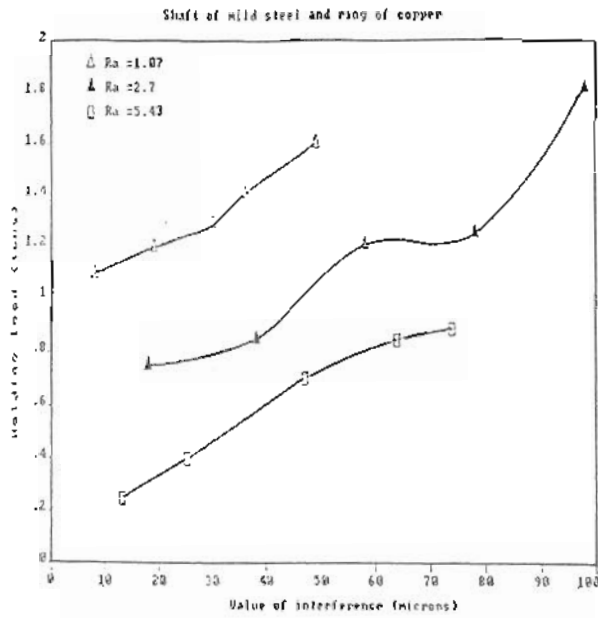


Fig. 5: Effect of the interference value on the H.L. of copper joints .

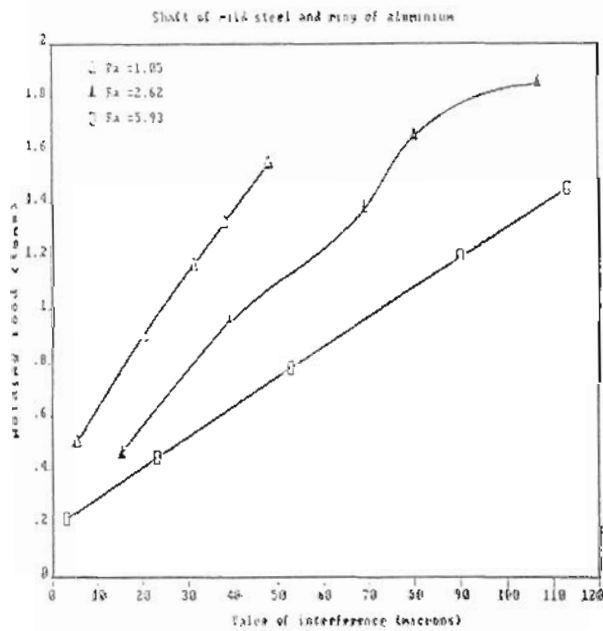


Fig. 6: Effect of the interference value on the H.L. of Aluminium joints .



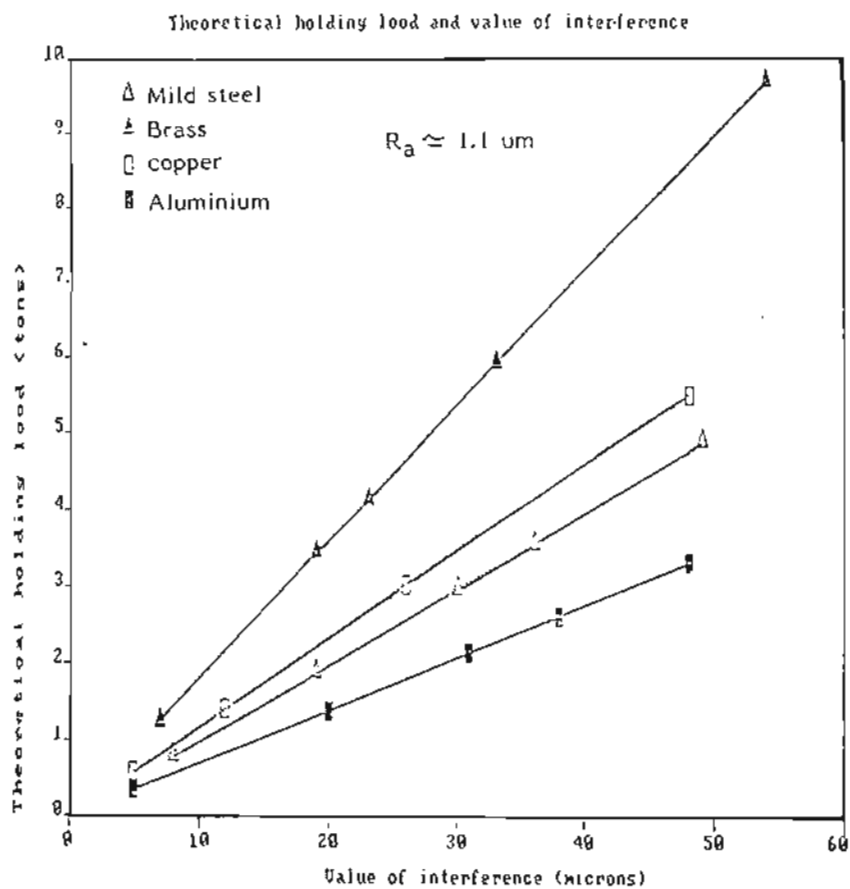


Fig. 7: Theoretical Holding load of different types of joints ( $R_a \approx 1.1 \mu m$ ).

Table 2-Shaft and ring of mild steel

Joint No.	shaft			ring			R <sub>a</sub> average $\mu$ m	$\mu_s$ average	value of interference $\mu$ m	Holding load in tons		% dev. of theor. H.L.
	R <sub>a</sub> $\mu$ m	$\epsilon^\circ$	$\lambda_a$ mm	R <sub>a</sub> $\mu$ m	$\epsilon^\circ$	$\lambda_a$ mm				Experimental	theoretical	
72 - 6	1.1	8.41	.046	0.95	7.40	0.046	1.02	0.324	7	1.52	1.25	+ 17
70 - 3	1.16	9.49	.043	0.98	8.10	0.048	1.07	0.327	19	2.6	3.44	- 32
71 - 1	1.21	7.13	.061	1.05	8.32	0.045	1.13	0.323	23	3.3	4.12	24
73 - 2	1.18	8.26	.051	0.99	7.90	0.045	1.08	0.324	33	4.5	5.92	31
74 - 7	1.15	7.82	.053	0.96	8.30	0.049	1.07	0.324	54	7.2	9.69	34
78 - 12	2.38	10.38	.081	2.36	8.60	0.109	2.50	0.33	7	0.81	1.28	58
76 - 10	2.29	10.58	.077	2.64	8.70	0.104	2.41	0.33	18	2.23	3.29	47
79 - 9	2.41	11.02	.077	2.58	9.78	0.094	2.49	0.333	28	3.42	5.16	50
77 - 13	2.31	11.19	.073	2.61	8.77	0.106	2.46	0.331	47	5.78	8.62	49
75 - 8	2.43	13.65	.062	2.52	8.04	0.113	2.47	0.334	60	7.4	11.11	50
82 - 17	5.43	11.39	.159	5.61	9.14	.213	5.52	0.332	11	0.99	2.02	104
80 - 20	5.38	15.11	.132	5.67	8.46	.239	5.52	0.337	21	1.98	3.92	96
84 - 19	5.35	14.75	.128	5.58	8.61	.232	5.46	0.336	32	3.21	5.90	83
81 - 18	5.46	14.46	.143	5.85	8.50	.246	5.65	0.336	42	4.45	7.82	75
83 - 21	5.37	13.50	.141	5.95	9.12	.233	5.66	0.335	54	5.73	10.02	75

Table - 3 - shaft of mild steel and ring of brass

Joint No.	shaft			ring			R <sub>a</sub> average μm	μ <sub>s</sub> average	value of inter- ference μm	Holding load in tons		% dev. of theor. H.L.
	R <sub>a</sub> μm	θ°	λ <sub>a</sub> mm	R <sub>a</sub> μm	θ°	λ <sub>a</sub> mm				Experimental	theoretical	
shaft-ring												
39 - 6	1.15	9.21	0.044	1.17	6.45	0.065	1.16	.324	5	1.03	0.58	43
2 - 1	1.23	8.58	0.051	1.33	8.48	0.056	1.28	.326	12	1.20	1.41	17
69 - 10	1.25	8.96	0.045	1.07	7.10	0.054	1.16	.324	26	1.50	3.04	102
42 - 11	1.23	9.88	0.044	1.18	6.73	0.062	1.20	.318	48	1.82	5.51	202
1 - 2	2.7	9.36	0.103	2.33	8.93	0.093	2.51	.328	12	0.9	1.42	57
8 - 7	2.8	13.4	0.074	2.6	8.94	0.104	2.70	.335	32	1.3	3.87	197
14 - 12	2.83	12.45	0.081	2.47	8.00	0.110	2.65	.332	38	1.4	4.55	225
7 - 4	2.98	11.98	0.088	2.50	8.42	0.106	2.72	.332	53	1.58	6.35	301
23 - 9	5.6	14.75	0.134	5.97	9.9	0.215	5.78	.339	5	0.1	0.61	500
30 - 8	5.33	15.12	0.124	5.27	8.5	0.221	5.30	.337	14	0.38	1.70	347
19 - 5	5.26	13.7	0.135	5.47	7.6	0.257	5.36	.333	32	0.77	3.85	400
64 - 3	5.17	13.5	0.135	5.83	10.5	0.198	5.50	.338	48	1.05	5.62	435



Table 4 - shaft of mild steel and ring of copper

Joint No.	shaft			ring			R <sub>a</sub> average $\mu$ m	$\mu$ S average	value of interference $\mu$ m	Holding load in tons		%dev. of theor. H.L.
	R <sub>a</sub> $\mu$ m	$\theta^\circ$	$\lambda_a$ mm	R <sub>a</sub> $\mu$ m	$\theta^\circ$	$\lambda_a$ mm				Experimental	theoretical	
13 - 24	1.03	6.3	0.058	0.88	6.06	0.052	0.95	0.318	8	1.08	0.786	27
3 - 10	1.32	7.3	0.065	0.85	5.56	0.055	1.08	0.319	19	1.19	1.87	57
9 - 23	1.25	7.6	0.059	0.95	7.55	0.045	1.10	0.322	30	1.28	2.98	132
47 - 19	1.30	7.3	0.064	0.99	5.78	0.061	1.14	0.320	36	1.40	3.56	154
35 - 20	1.23	7.25	0.061	0.96	7.62	0.045	1.09	0.322	49	1.60	4.87	204
10 - 12	2.37	11.06	0.076	2.93	10.7	0.097	2.65	0.334	18	0.75	1.85	146
43 - 4	2.25	11.53	0.069	2.87	9.1	0.112	2.56	0.332	38	0.85	3.89	357
38 - 21	2.76	10.5	0.093	2.90	11.7	0.088	2.83	0.337	58	1.20	6.04	403
58 - 5	2.83	11.3	0.089	2.89	10.4	0.099	2.86	0.334	78	1.25	8.05	544
61 - 6	2.37	11.8	0.071	2.89	11.4	0.090	2.63	0.337	98	1.81	10.20	463
27 - 3	5.85	12.64	0.163	5.02	10.50	0.170	5.43	0.336	13	0.25	1.34	436
18 - 14	5.23	14.80	0.124	5.77	9.95	0.206	5.50	0.339	25	0.40	2.62	555
54 - 8	5.57	13.60	0.45	5.14	9.80	0.187	5.35	0.337	47	0.70	4.90	600
26 - 11	5.42	13.70	0.140	5.13	9.90	0.185	5.27	0.338	64	0.85	6.68	685
51 - 1	5.13	14.10	0.128	5.97	9.20	0.231	5.55	0.338	74	0.89	7.73	768

Table 5 - shaft of mild steel and ring of Aluminium

Joint No.	shaft			ring			R <sub>a</sub> average µm	R <sub>s</sub> average	value of inter- ference µm	Holding load in tons		% dev. of theor. H.L.
	R <sub>a</sub> µm	θ°	λ <sub>a</sub> mm	R <sub>a</sub> µm	θ°	λ <sub>a</sub> mm				Experimental	theoretical	
4 - 20	0.92	7.77	0.042	0.98	4.75	0.074	0.95	0.319	5	0.50	0.347	30
17 - 23	1.30	6.89	0.068	0.79	5.90	0.048	1.05	0.320	20	0.90	1.39	54
5 - 21	1.22	6.79	0.064	0.94	6.80	0.050	1.08	0.320	31	1.16	2.15	85
6 - 24	1.33	6.77	0.070	0.83	5.10	0.058	1.08	0.318	38	1.32	2.63	99
40 - 22	1.35	6.69	0.072	0.85	5.42	0.056	1.10	0.318	43	1.54	3.32	117
12 - 5	2.49	10.13	0.087	2.19	9.72	0.080	2.34	0.308	15	0.46	1.01	119
31 - 4	2.90	10.15	0.102	2.18	10.48	0.074	2.54	0.332	39	0.95	2.82	196
55 - 1	3.18	9.99	0.113	2.58	9.89	0.093	2.88	0.331	69	1.37	4.97	262
56 - 3	3.20	9.78	0.117	2.19	10.62	0.074	2.68	0.332	80	1.65	5.78	250
57 - 2	3.05	9.99	0.109	2.28	10.06	0.081	2.66	0.331	107	1.85	7.71	316
34 - 17	5.65	14.88	0.134	6.57	8.51	0.275	6.11	0.3375	3	0.22	0.22	0
21 - 10	6.40	15.10	0.149	6.13	7.60	0.288	6.26	0.336	23	0.45	1.68	266
59 - 13	6.15	15.10	0.143	5.47	8.50	0.230	5.81	0.3375	53	0.79	3.89	392
62 - 8	5.47	15.13	0.127	5.76	7.35	0.280	5.61	0.336	90	1.20	6.58	448
60 - 14	5.22	15.00	0.122	6.53	7.72	0.302	5.87	0.336	113	1.45	8.26	469